Journal of Molecular Graphics and Modelling 28 (2009) 37–45

Contents lists available at ScienceDirect

Journal of Molecular Graphics and Modelling

journal homepage: www.elsevier.com/locate/JMGM

Theoretical studies on the interaction of modified pyrimidines and purines with purine riboswitch

Baoping Ling [a], Zhiguo Wang [a,b], Rui Zhang [a,b], Xianghua Meng [a,c], Yongjun Liu [a,b,*], Changqiao Zhang [a], Chengbu Liu [a,**]

[a] School of Chemistry and Chemical Engineering, Shandong University, Jinan, Shandong 250100, China
[b] Northwest Institute of Plateau Biology, Chinese Academy of Sciences, Xining, Qinghai 810001, China
[c] Department of Chemistry, Qufu Nornal University, Qufu, Shandong 273165, China

ARTICLE INFO

Article history:
Received 3 February 2009
Received in revised form 18 March 2009
Accepted 21 March 2009
Available online 31 March 2009

Keywords:
Pyrimidine
Purine
Purine riboswitch
Docking
Molecular dynamics

ABSTRACT

Recent experimental study [S.D. Gilbert, S.J. Mediatore, R.T. Batey, Modified pyrimidine specifically bind the purine riboswitch, J. Am. Chem. Soc. 128 (2006) 14214–14215] demonstrated that the purine riboswitch could specifically bind some ligands other than purines such as amino-pyrimidines, and the authors proposed that the five-membered ring of purine was not required for recognition. To get insight into the interaction details, we used molecular docking method to investigate the interactions of a mutant form of guanine riboswitch with a series of amino-purines, amino-pyrimidines and imidazole derivatives, and employed molecular simulation method to study the dynamic behavior of the selected complexes. The calculation results reveal that (1) all the amino-purines and amino-pyrimidines bind in a same cavity composed of four nucleobases including U22, U47, U51 and U74, which is consistent with the experimental results, while the two imidazole derivatives adopt other binding modes; (2) the purines are engulfed within three-way junction motifs, but most pyrimidines only form two-way junctions with the riboswitch; (3) the number and position of amino substituents could seriously affect the binding of pyrimidines. As riboswitches are potentially excellent candidates for antibiotic therapeutics, these findings may be useful for understanding the range of compounds that riboswitch can specifically recognize.

1. Introduction

Riboswitches are structured elements within the 5′-untranslated regions of messenger RNA. It can specifically bind small molecular metabolites to regulate gene expression in virtue of its conformational changes without the need of protein cofactors [1]. Breaker and co-workers [2] firstly discovered the natural riboswitch and demonstrated that some messenger RNAs contain natural aptamer domain. In recent years, over ten distinct riboswitches have been characterized that can recognize different metabolites, including vitamin [3], amino acid [4] and purine nucleotides [5–7]. Riboswitches contain an aptamer domain and an expression platform. The aptamer domain is responsible for ligand binding, and the expression platform transmits the ligand-binding state of the aptamer domain through conformational change [8–10].

The purine riboswitch is one of the smallest known riboswitches so far. Despite binding different metabolites, the purine riboswitch has quite similar secondary and tertiary structures and recognizes ligands by hydrogen bonding or Van der Waals interactions. Mandal et al. [11] observed that the G-box domain in mRNA 5′-UTR of *B. subtilis xpt-pbuX* could serve as an aptamer domain for guanine and related purines, and exhibits high affinity and selectivity for guanine. The alteration of every functional position on the guanine heterocycle could cause a substantial loss of binding energy. Recently, Batey et al. [12] solved the structure of guanine-responsive riboswitch (aptamer domain) bound to hypoxanthine by X-ray crystallography. The result showed that, in the hypoxanthine-bound state, the highly conserved nucleotides adopted a three-dimensional fold to create a binding pocket, in which the ligand was almost completely enveloped by Watson–Crick interaction. Serganov et al. [13] determined the crystal structures of adenine and guanine riboswitches with X-ray crystallography. Although the adenine and guanine riboswitches only shared 60% sequence identity, they formed nearly identical

* Corresponding author at: School of Chemistry and Chemical Engineering, Shandong University, Jinan, Shandong 250100, China. Tel.: +86 531 883 655 76; fax: +86 531 885 644 64.
** Corresponding author.
E-mail address: yongjunliu_1@sdu.edu.cn (Y. Liu).

1093-3263/$ – see front matter © 2009 Elsevier Inc. All rights reserved.
doi:10.1016/j.jmgm.2009.03.005

binding pockets for their corresponding ligands. Gilbert et al. [14] analyzed the detailed structures of the guanine and adenine riboswitches and found that the aptamer domain of the purine riboswitch contained a pyrimidine residue (Y74) which formed a Watson–Crick base-pairing interaction with the bound purine ligand and discriminated between adenine and guanine. If this pyrimidine was U74, the purine riboswitch could specifically recognize adenine; if this residue mutated to C74, the riboswitch would convert its specificity from adenine to guanine.

From theoretical point of view, Schneider and Sühnel [15] reported the molecular dynamics simulation of flavin mononucleotide (FMN) interacting with RNA aptamer. Their calculations predicted that the flexible phosphoglycerol moiety of FMN moved toward to G27 and formed hydrogen bonds with the nucleobases. Nguyen et al. [16] performed ab initio calculations to explore the geometrical structure and charge distribution before and after malachite green (MGA) complexes with RNA. They found that the uneven charge distribution in the binding pocket provided the major contribution for the structural change of the ligand. Dieckmann et al. [17] used molecular modeling to evaluate how well the base substitutions fitted into the structural framework of the original ATP-binding structure.

These experimental and theoretical results exemplified that the aptamer complexes with the ligands mainly by Watson–Crick base pair or hydrogen-bond interactions. When the functional groups of ligand change or the conserved nucleotides of the aptamer mutate, the interactions and the binding affinities will change correspondingly.

Although molecular dynamics simulations have been reported about the aptamers interacting with small metabolites [15,18–21], and some crystal structures of natural riboswitches complexing with different metabolites have been solved [5,6,22,23], theoretical studies on the interaction mechanism are still very limited. Gilbert et al. validated experimentally that aminopyrimidines were also able to specifically bind to the aptamer domain of the purine riboswitch GR(C74U) [6] and proposed that the five-membered ring of purine was not required for recognition, the six-membered ring was the primary recognition determinant.

On the basis of Gilbert's experiments, this paper investigates the interactions of a mutant form of guanine riboswitch GR(C74U) with series of amino modified pyrimidines, purines and imidazole derivatives by using molecular docking and dynamic simulation. The binding mode of different ligands, and how the number and

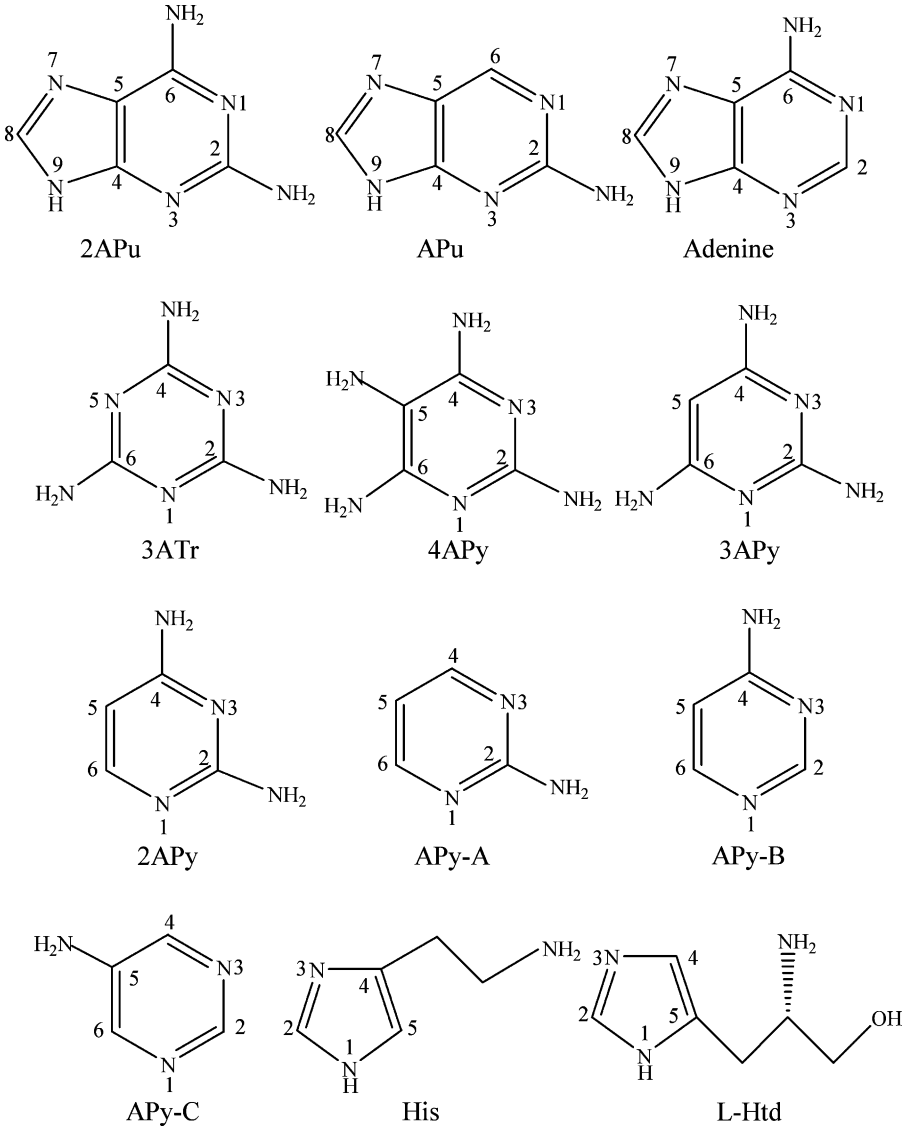

Fig. 1. Structures of the selected ligands for docking.

position of the substituents will affect the interactions are included.

2. Methods

We focus on the studies on the interactions between the riboswitch and purines as well as pyrimidines bearing amino groups. To compare the calculation results with experimental data, except one purine (APu) and three pyrimidines (APy-A, APy-B and APy-C) were designed by ourselves, all the other ligands, two purines (2APu and adenine), three pyrimidines (4APy, 3APy and 2APy), 2,4,6-triamino-1,3,5-triazine (3ATr) and two imidazole derivatives, were selected from Gilbert's experiments [6]. The structures of the ligands are shown in Fig. 1. GR(C74U) was taken from Brookhaven Protein Data Bank with the PDB code of 2G9C.

All the structures of the ligands were optimized using Gaussion03 program [24] at the level of B3LYP/6-31g(d). PDB ID of 2G9C was the crystal structure of the complex GR(C74U)/3APy. Before calculation, except the receptor, all the other substances were firstly removed from the crystal structure, then AutoDock program was applied to add polar hydrogen atoms and Kollman United Atom Charges to the receptor.

2.1. Docking

Based on the empirical binding free energy function and Lamarckian genetic algorithm, version 4.0 of the program AutoDock [25] was used for the receptor and ligand docking. Grid module was employed to create grid maps with $80 \times 80 \times 80$ points and a grid-point spacing of 0.0375 nm. The centroid of four special nucleobases including U22, U47, U51 and U74 was used as the center of the box. For each complex, 50 independent docking runs were conducted. The settings of parameters were as follows [26–28]: population size of 150, a maximum number of 25 million energy evaluations, a maximum number of generations of 27,000, a crossover rate of 0.8 and a mutation rate of 0.02 were set up. For the local search, the pseudo Solis & Wets method was applied, using a maximum number of 300 iterations, the probability of performing a local search on an individual in the same population was 0.06, and the maximum number of consecutive success or failures before doubling or halving the local search step size was 4. When docking, GR(C74U) was set rigid, while all the torsional bonds of ligands were set free. The docking results were clustered according to a root-mean-square deviation (RMSD) criterion of 0.1 nm and evaluated depending on the binding free energy.

2.2. Molecular dynamics simulation

GROMACS program has been successfully used to perform molecular dynamics (MD) simulation of RNA [29,30]. In this paper, we employed the same method to perform MD simulation.

The docking results were used as the starting structures for MD simulation. In calculation, the complex was placed in a cubic box center of 7.9 nm × 7.9 nm × 7.9 nm with period boundary conditions, and solvated by TIP3P water molecules. K^+ counterions were added to maintain overall system electroneutrality. The simulation was performed with GROMACS 3.3.1-1 suite program [31] using AMBER99 force field [32–35]. The Berendsen temperature coupling was used to keep the system at 300 K, and the constant of coupling was 0.1 ps; The Parrinello-Rahman pressure coupling was employed to control the constant pressure at 1 bar with the coupling constant of 0.5 ps. The partial mesh Ewald (PME) algorithm was applied to calculate long-range electrostatics interactions with a cutoff of 0.9 nm, and a cutoff of 1.4 nm was set for Van der Waals interactions. The Verlet leapfrog integrator with an integration time step of 2 fs was used, and LINCS algorithm was employed to keep all bonds involving hydrogen atoms rigid. Firstly, the system was subjected to 2500 steps of steep descent energy minimization; the position restrained molecular dynamics was subsequently carried out for 150 ps, and harmonic restraints with force constant of 1000 kJ/(mol nm^2) were applied to maintain the conformations of the riboswitch and the ligand close to their initial structures; finally, after all the restraints were removed, the MD simulation was run for 4 ns to the whole system [36,37]. Time step was set to 2 fs, and the trajectory was collected as a series of snapshots saved every 1 ps [20].

3. Results and discussion

3.1. Docking

From the docking results, we find that for each ligand of purines and pyrimidines, the 50 independent runs are almost clustered into one group, and the difference of binding energies in each group is very small (the maximum value is only 0.07 kcal/mol), suggesting actually only one binding mode for each ligand. Besides RMSD clustering, AutoDock ranks the conformations in terms of binding energies. The conformation with the lowest energy serves as the starting structure for the following MD simulation [38]. In addition, the intermolecular energy (which is a combination of van der Waals energy, hydrogen bonding energy, desolvation energy and electrostatic energy) and torsional energy can be obtained. The

Table 1
Diverse energies (kcal/mol) of GR(C74U) complexes with the ligands calculated by docking.

Ligands	vdw + Hbond + desolv. energy	Electrostatic energy	Torsional energy	Binding energy	Experimental[a] ΔG	Binding energy[b] ΔE
3ATr	−4.35	−6.52	0.00	−10.87	−6.5	−39.36
4APy	−6.33	−2.32	0.82	−7.83	−6.5	−41.63
3APy	−5.57	−2.32	0.55	−7.34	−6.6	−36.67
2APy	−5.16	−2.23	0.27	−7.12	–	−29.84
APy-A	−4.54	−2.24	0.27	−6.51	–	−23.82
APy-B	−4.25	−0.13	0.27	−4.09	–	−24.62
APy-C	−4.14	−0.09	0.27	−3.96	–	−17.94
2APu	−6.47	−2.39	0.27	−8.59	−11.0	−47.53
APu	−6.06	−2.31	0.00	−8.37	–	−39.40
Adenine	−5.67	−0.19	0.00	−5.86	−8.8	−42.54
His-1	−3.58	−4.07	0.82	−6.83		
His-2	−4.54	−3.06	0.82	−6.78		
LHtd-1	−4.67	−4.46	1.37	−7.76		
LHtd-2	−4.53	−4.57	1.37	−7.73		
LHtd-3	−4.63	−4.46	1.37	−7.72		

[a] The experimental data are from Ref. [6]. For histamine and L-histidinol, no detectable binding was observed.
[b] The binding energies calculated at B3lyp/6-31g(d) level, where $\Delta E = E_{complex} - (E_{base} + E_{ligand})$.

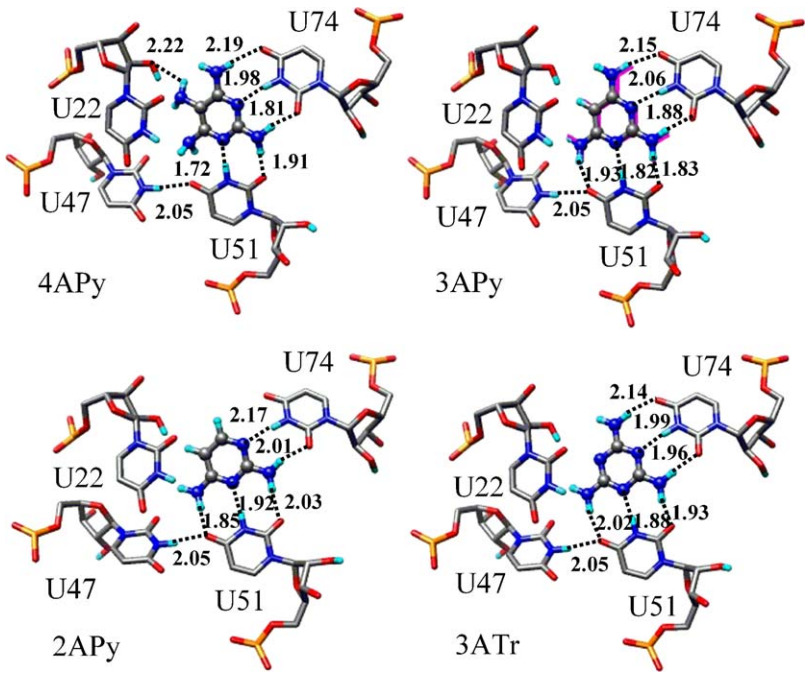

Fig. 2. Docking conformations of GR(C74U) complexes with pyrimidines bearing 2–4 amino groups. The dashed lines show the hydrogen bonds with lengths in 0.1 nm. For 3APy, the ball and stick model is for the docking conformation while the stick model in magenta is for the crystal structure.

sum of intermolecular energy and torsional energy is binding energy. Because the torsional energy is very small, the intermolecular energy is the dominant item for binding energy (see Table 1).

Fig. 2 shows the docking results of 4APy, 3APy, 2APy and 3ATr bound to the riboswitch. For comparison, the superimposition of the docking conformation and crystal structure of 3APy is also shown in Fig. 2. We can see that the two structures are almost identical in the binding pocket. The RMSD value between these two structures is only 0.047 nm, suggesting the molecular docking can reproduce the crystal structure very well. Fig. 2 also shows that the four pyrimidine derivatives are located in a same binding pocket and their orientations are almost identical. These ligands form stable complexes with the riboswitch by hydrogen bonding with U51 and U74, i.e., the Watson–Crick interactions of the pyrimidine rings with U51 and U74 fix the backbone of pyrimidines.

Table 1 shows that from 4APy to 2APy the binding energies increase gradually, which means the amino groups could facilitate

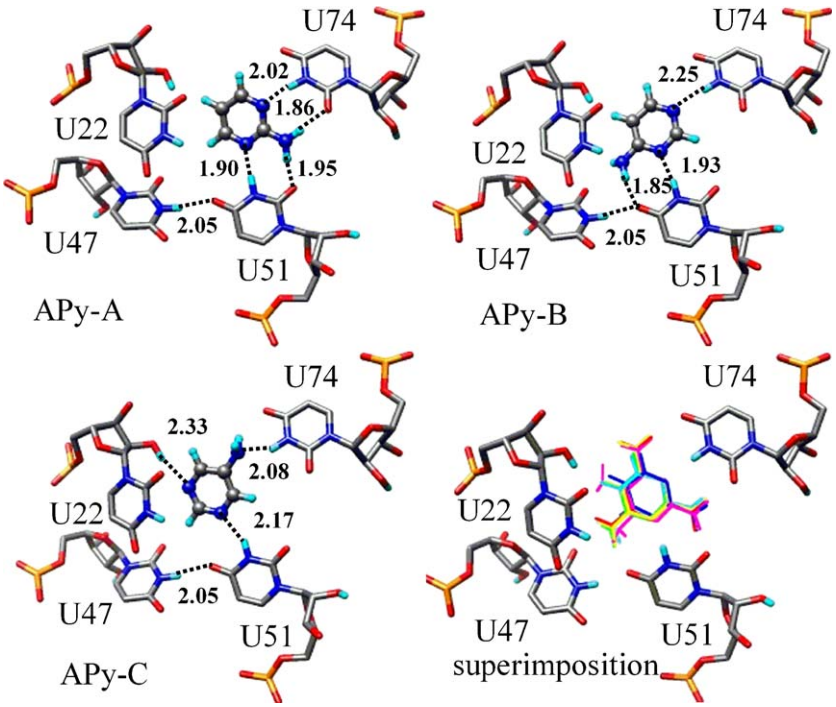

Fig. 3. Docking conformations of GR(C74U) complexes with pyrimidines bearing one amino group and the superimposition of several pyrimidines and 3ATr in the binding pocket: red for 3ATr, yellow for 3APy, magenta for 4APy, cyan for 2APy, green for APy-A and blue for APy-B. The dashed lines show the hydrogen bonds with lengths in 0.1 nm.

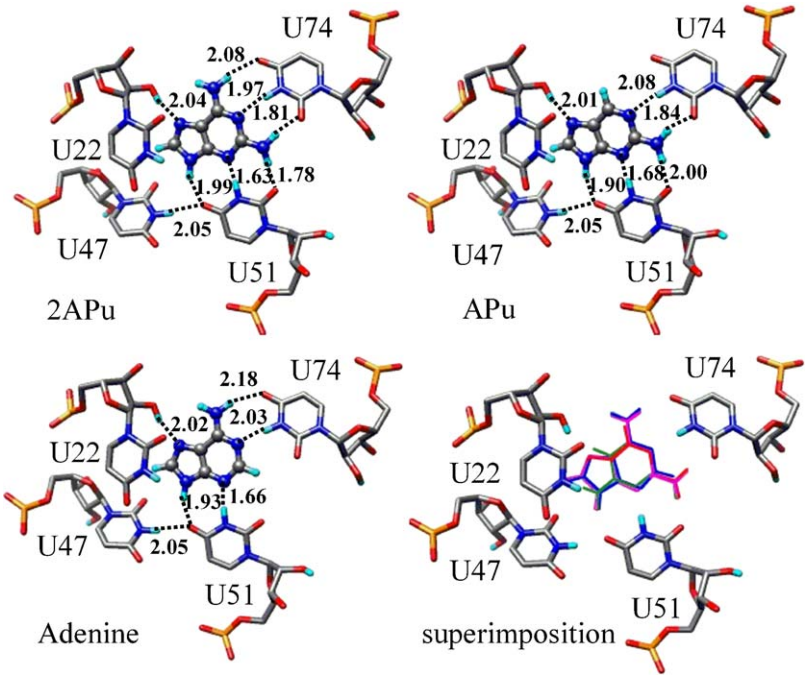

Fig. 4. Docking conformations of GR(C74U) complexes with purines ligands and superimposition of three purines and 3APy in the binding pocket: blue for 2APu, red for APu, green for adenine, yellow for 3APy. The dashed lines show the hydrogen bonds with lengths in 0.1 nm.

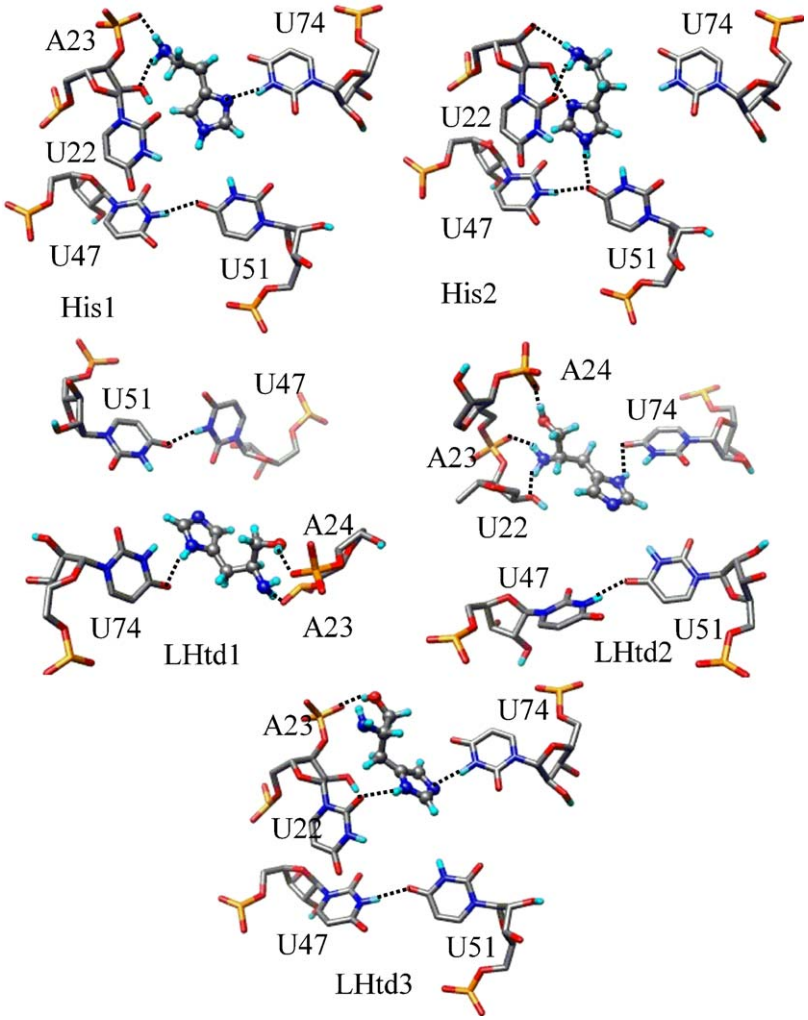

Fig. 5. Docking conformations of GR(C74U) complexes with histamine and L-histidinol.

the binding of pyrimidine to GR(C74U). We also notice that the binding energy of 3ATr is very low. The reason is 3ATr has special electric structure and its electrostatic interaction with GR(C74U) is much lower than that of other pyrimidines (−6.52 *vs* −2.32 kcal/mol) (see Table 1).

We also performed molecular docking with pyrimidines bearing only one amino group, the docking conformations are shown in Fig. 3. We can see that the three ligands are still held in the same binding pocket, but the hydrogen bonds with U74 and U51 are different from that of 4APy, 3APy, 2APy and 3ATr: APy-A forms totally four hydrogen bonds with U74 and U51, APy-B and APy-C only form three and two hydrogen bonds with U74 and U51, respectively. The three ligands seem "too small" in the binding pocket. The binding energy of APy-A is −6.51 kcal/mol, and that of APy-B and APy-C are only −4.09 and −3.96 kcal/mol, respectively. From the binding energy point of view, we can deduce that GR(C74U) could only specifically bind pyrimidine with at least two amino groups and one amino group should be at 2-position.

Fig. 4 gives the docking conformations of 2,6-diaminopurine (2APu), 2-aminopurine (APu) and adenine. Compared with pyrimidine, besides form hydrogen bonds with U51 and U74 by the pyrimidine ring, the five-membered ring of purine also forms hydrogen bond with U22. 2APu forms totally seven hydrogen bonds with the surrounding nucleotides. APu and adenine form six and five hydrogen bonds with GR(C74U), respectively. The superimposition of the three amino-purines and 3APy is also given in Fig. 4. The backbones of the four ligands are superimposed together and the six-membered rings of purines fully overlap with the pyrimidine ring of 3APy.

By comparing Figs. 2 and 4, one can see that most hydrogen bonds are formed between the pyrimidine ring and U74 and U51. The five-membered rings of purines only form two hydrogen bonds with the nucleotides. In addition, the binding energies of pyrimidines with more than two amino groups are only slightly smaller than that of 2APu and APu. Adenine corresponds to the largest binding energy because no amino group at 2-posiyion. So, we can confirm Gilbert's suggestions that the five-membered ring of purines provides minor contribution to the recognition, the six-membered ring of the ligand is the primary recognition determinant [6].

For comparison, this paper also studies the interactions of GR(C74U) with two imidazole derivatives, histamine (His) and L-histidinol (L-Htd), as shown in Fig. 5. Histamine binds to GR(C74U) with two modes: His1 and His2. In His1, only one hydrogen bond is formed with U74. In His2, no hydrogen bond is formed with U74. L-histidinol binds to GR(C74U) with three modes: LHtd1, LHtd2 and LHtd3. In these three binding modes, only one hydrogen bond is formed with U74 and the binding pockets are totally different from that of pyrimidine derivatives. In fact, these two imidazole derivatives displayed no detectable binding as reported by Gilbert et al. [6]. Accordingly, the binding modes shown in Fig. 5 are meaningless for recognition.

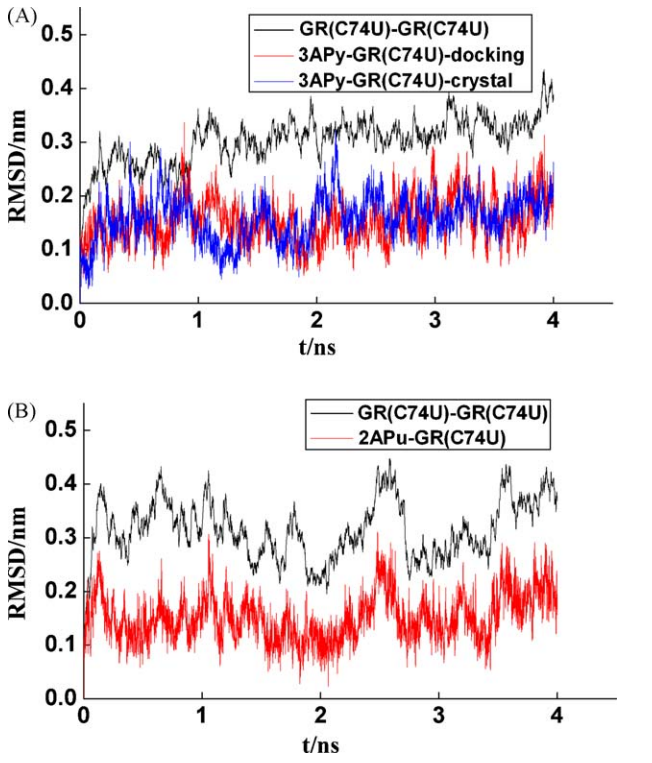

Fig. 6. Time dependences of RMSDs (nm) from MD simulation. (A) GR(C74U) relative to its starting structure (black), 3APy relative to GR(C74U) (red) in the docking structure, and 3APy relative to GR(C74U) (blue) in the crystal structure. (B) GR(C74U) relative to its starting structure (black), 2APu relative to GR(C74U) (red) in the docking structure.

To get more accurate interaction energies between nucleotides and the ligands, quantum calculation were carried out by using density functional theory (DFT). In our calculation, only the four bases that can form hydrogen bonds with ligands were included. The geometries of the ligands were fully optimized and the structures of the nucleobases were fixed. All the energies were calculated at the level of B3LYP/6-31g(d). The calculated energies of ΔE [$\Delta E = E_{complex} - (E_{base} + E_{ligand})$] are listed in Table 1.

Table 1 indicates that the binding energies calculated at B3LYP/6-31g(d) level display very similar tendency as those of docking results. Pyrimidine and purine derivatives correspond to the lower binding energies than that of APy-A, APy-B and APy-C, i.e., GR(C74U) can only specifically bind pyrimidine and purine derivatives with at least one amino group at 2-position.

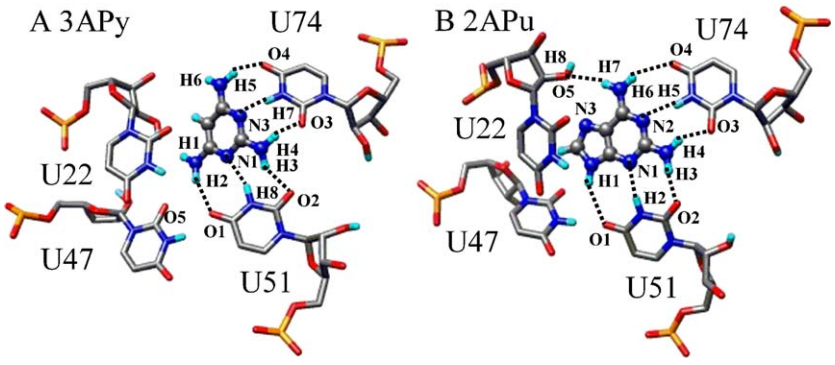

Fig. 7. Hydrogen bonds arrangements in average structure obtained by MD simulation. (A) 3APy with U51 and U74. (B) 2APu with U22, U51 and U74.

3.2. Molecular dynamics simulations

GROMACS 3.3.1-1 suite program was used to investigate the conformational changes and dynamics characteristic of the riboswitch complexes with ligands.

For the complex of GR(C74U) with 3APy, both of the crystal structure and docking conformation were used as the initial structures for MD simulation. The time dependences of RMSDs are shown in Fig. 6A. The RMSD of GR(C74U) relative to its initial structure shows that GR(C74U) reaches equilibrium after 1 ns with the RMSD value of 0.3 nm. The RMSD of the ligand (3APy) relative to GR(C74U) shows that their relative position changes slightly, since the RMSD value is always maintained at 0.15 nm during the whole MD simulation. In particular, the RMSD curve of the crystal structure agrees well with that of the docking result, suggesting the docking structure is reliable.

Fig. 7A gives the hydrogen bonds arrangements between 3APy and nucleotides in the average structure obtained by MD simulations. The time courses of the important hydrogen bonds obtained from the dynamic trajectory are shown in Fig. 8.

From Fig. 8, one can see that 3APy forms six stable hydrogen bonds with U51 and U74. But their time courses display different characteristic. Fig. 8A–C are the time courses of the three hydrogen bonds between 3APy and U51. In Fig. 8A, at the simulation time from 0 to 2 ns, the hydrogen bond length fluctuates at ~0.35 nm and finally stabilizes at 0.20 nm. It is because the starting structure was based on the docking results and underwent an energy minimization step before simulation. During the energy minimization, the amino group was rotated. The stable time course shown in Fig. 8B indicates that the nitrogen atom of the pyridine ring of the ligand forms strong hydrogen bond with the backbone of U51. The time course of hydrogen bond between H3 atom of 3APy and U51 shows a strong fluctuation because the amino group is rotatable.

Fig. 8D–F are the time courses of the three hydrogen bonds between 3APy and U74. The three hydrogen bonds are also stable during the whole MD simulation. For the same reason that the amino group can rotate during the simulation, Fig. 8D and F shows stronger fluctuation than that of Fig. 8E. Fig. 8C and F corresponds to the same amino group, so their fluctuations are correlative.

In addition, MD simulations were also performed for 2APu. The time dependences of RMSDs are shown in Fig. 6B. The RMSD of GR(C74U) relative to its starting structure is little larger than that of 3APy complex, which indicates that the structure of GR(C74U) underwent relative lager changes upon the binding of 2APu. We ascribe it to the different structure of 3APy and 2APu. But the RMSD of 2APu relative to GR(C74U) is basically stable at 0.18 nm, suggesting that 2APu could bind strongly to the riboswitch.

By comparing the average structure obtained by MD simulation (Fig. 7B) with that of the docking result (Fig. 4), one can see that 2APu always forms hydrogen bonds with U74 and U51. But the hydrogen bond with H8 (U22) was replaced by a new one {O5 (U22) with H7 (2APu)}. We noted that the hydrogen bonds between 2APu and the nucleobases (U74 and U22) are slightly lengthened. We refer it to the repulsion between U22 and the five-membered ring of 2APu that makes their relative position changes.

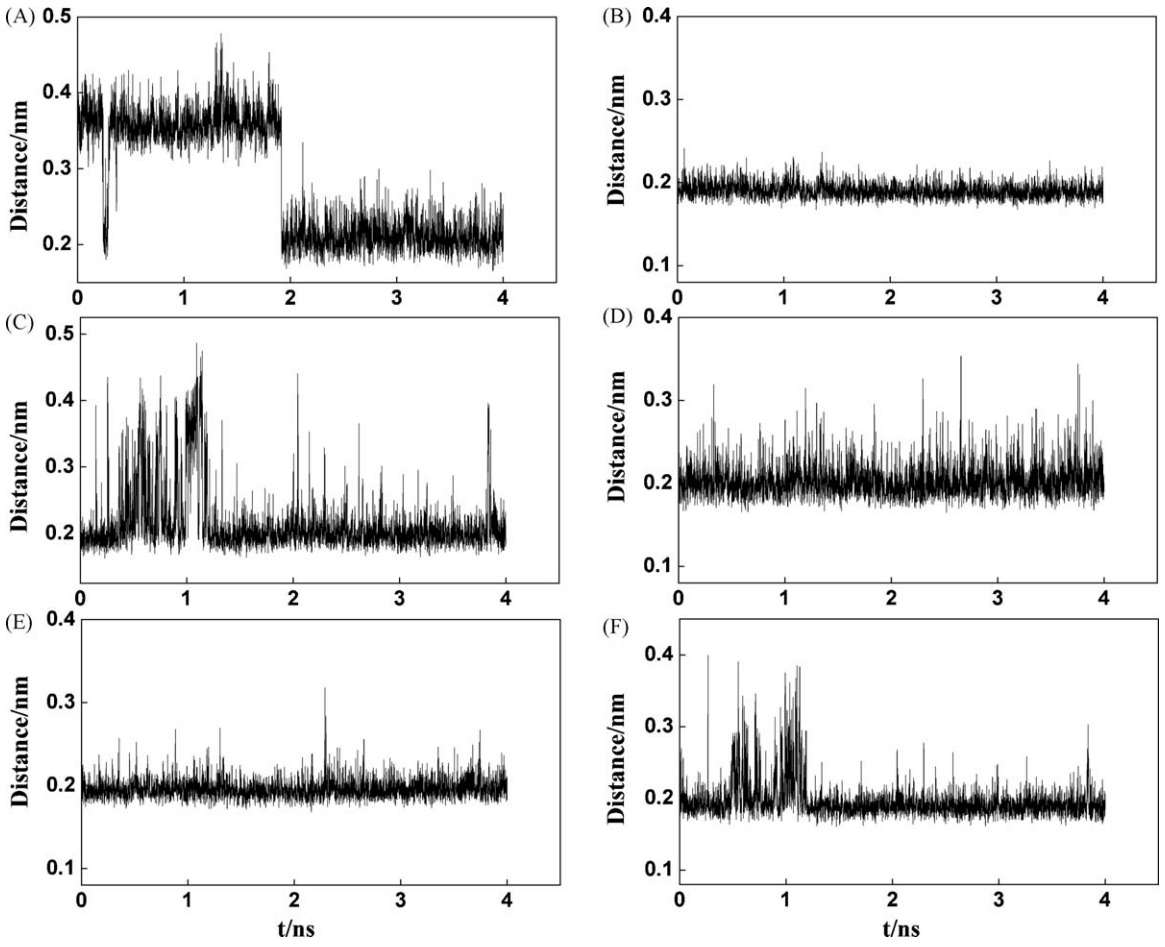

Fig. 8. Time courses of hydrogen bond lengths in nanometer between 3APy and U51, U74: (A) U51H8···N1; (B) U51O2···H3; (C) U51O1···H2; (D) U74H7···N3; (E) U74O4···H5; (F) U47O5···H1.

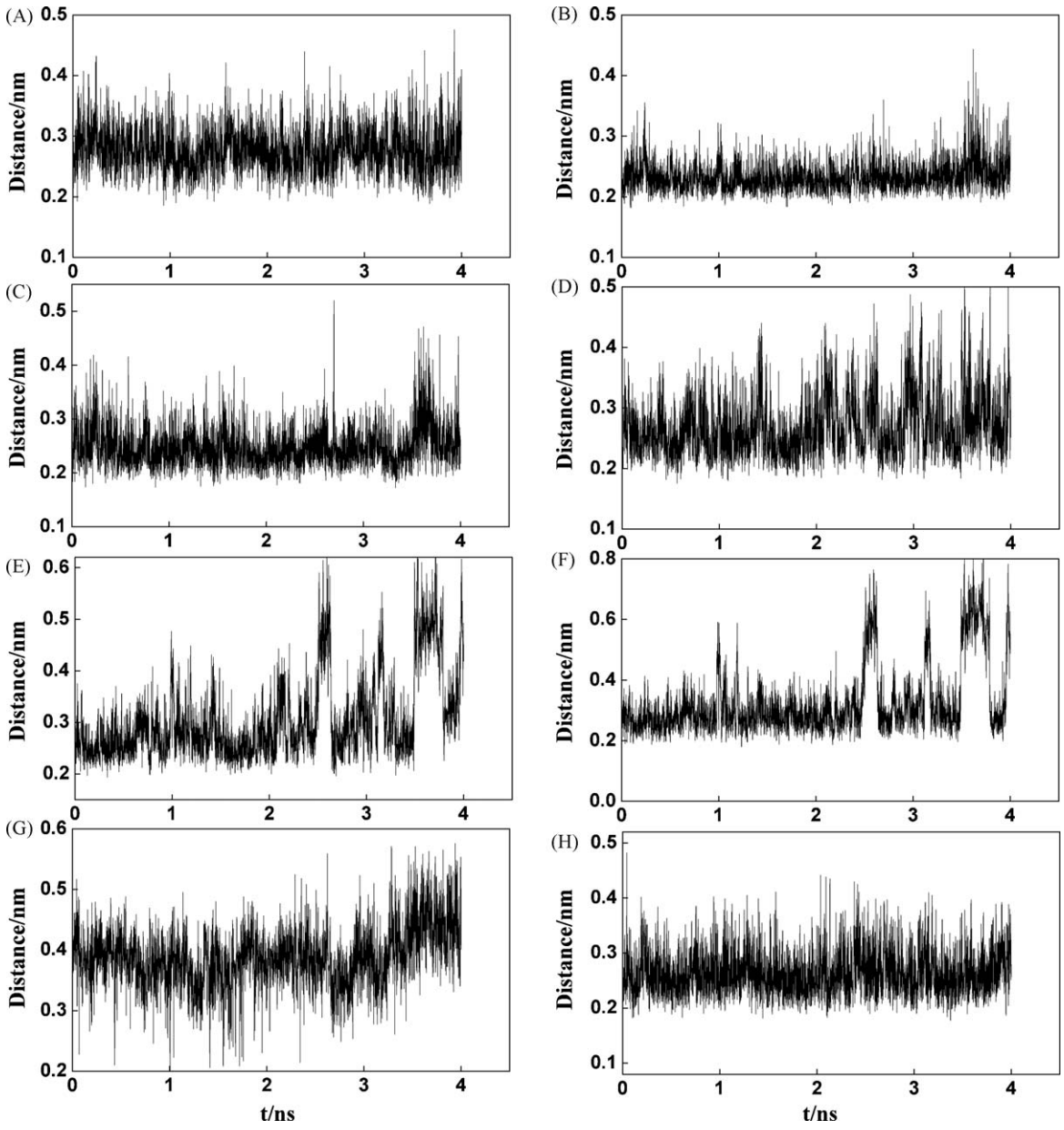

Fig. 9. Time courses of hydrogen bond lengths in nanometer between 2APu and U51,U74 and U22: (A) U51O1···H1; (B) U51H2···N1; (C) U51O2···H3; (D) U74O3···H4; (E) U74H5···N2; (F) U74O4···H6; (G) U22H8···N3; (H) U22O5···H7.

According to the dynamic trajectory, the time courses of hydrogen bond lengths between 2APu and GR(C74U) can be drawn. Fig. 9 shows that the ligand forms stable hydrogen bonds with U74 and U51.

From the MD simulations, we can deduce that the pyrimidine ring of the ligand forms strong Watson–Crick interaction with U74 and U51 no matter the ligand is pyrimidine or purine, which is the basis for the molecular recognition.

4. Conclusion

We have studied the interaction details of the purine riboswitch (GR(C74U)) with series of amino-purines, amino-pyrimidines and imidazole derivatives by using molecular docking and the dynamic features of two complexes of GR(C74U) with 3APy and 2APu by MD simulation. The calculation results reveal that all the amino-purines and amino-pyrimidines bind to the purine riboswitch GR(C74U) in a same pocket, but the two imidazole derivatives locate at different binding sites with multiple binding modes; the number and position of amino substituents can seriously affect the binding affinity, at least one amino group is required at 2-position of pyrimidine for forming Watson–Crick interaction with U74 and U51. By comparing the binding energies and modes, we can confirm that the six-membered rings of the purine and pyrimidines are the primary recognition determinant.

Acknowledgements

This work is supported by the grant from the Major State Research Development Programs (No. 2008CB13617508) and National Science Foundation of China (Nos. 20633060 and 30873158).

References

[1] G. Mayer, M.L. Raddatz, J.D. Grunwald, M. Famulok, RNA ligands that distinguish metabolite-induced conformations in the TPP riboswitch, Angew. Chem. Int. Ed. 46 (2007) 557–560.

[2] W. Winkler, A. Nahvi, R.R. Breaker, Thiamine derivatives bind messenger RNAs directly to regulate bacterial gene expression, Nature 419 (2002) 952–956.
[3] A. Nahvi, J.E. Barrick, R.R. Breaker, Coenzyme B_{12} riboswitches are widespread genetic control elements in prokaryotes, Nucl. Acids Res. 32 (2004) 143–150.
[4] M. Mandal, M. Lee, J.E. Barrick, Z. Weinberg, G.M. Emilsson, W.L. Ruzzo, R.R. Breaker, A glycine-dependent riboswitch that uses cooperative binding to control gene expression, Science 306 (2004) 275–279.
[5] S.D. Gilbert, C.E. Love, A.L. Edwards, R.T. Batey, Mutational analysis of the purine riboswitch aptamer domain, Biochemistry 46 (2007) 13297–13309.
[6] S.D. Gilbert, S.J. Mediatore, R.T. Batey, Modified pyrimidine specifically bind the purine riboswitch, J. Am. Chem. Soc. 128 (2006) 14214–14215.
[7] M. Mandal, R.R. Breaker, Gene regulation by riboswitches, Nat. Rev. Mol. Cell Biol. 5 (2004) 451–463.
[8] W.C. Winkler, R.R. Breaker, Genetic control by metabolite-binding riboswitches, ChemBioChem 4 (2003) 1024–1032.
[9] R. Rieder, K. Lang, D. Graber, R. Micura, Ligand-induced folding of the adenosine deaminase A-riboswitch and implications on riboswitch translational control, ChemBioChem 8 (2007) 896–902.
[10] H. Schwalbe, J. Buck, B. Fürtig, J. Noeske, J. Wöhnert, Structures of RNA switches: insight into molecular recognition and tertiary structure, Angew. Chem. Int. Ed. 46 (2007) 1212–1219.
[11] M. Mandal, B. Boese, J.E. Barrick, W.C. Winkler, R.R. Breaker, Riboswitches control fundamental biochemical pathways in *Bacillus subtilis* and other bacteria, Cell 113 (2003) 577–586.
[12] R.T. Batey, S.D. Gilbert, R.K. Montange, Structure of a natural guanine-responsive riboswitch complexed with the metabolite hypoxanthine, Nature 432 (2004) 411–415.
[13] A. Serganov, Y.R. Yuan, O. Pikovskaya, A. Polonskaia, L. Malinina, A.T. Phan, C. Hobartner, R. Micura, R.R. Breaker, D.J. Patel, Structure basis for discriminative regulation of gene expression by adenine- and guanine-sensing mRNAs, Chem. Biol. 11 (2004) 1729–1741.
[14] S.D. Gilbert, C.D. Stoddard, S.J. Wise, R.T. Batey, Thermodynamic and kinetic characterization of ligand binding to the purine riboswitch aptamer domain, J. Mol. Biol. 359 (2006) 754–768.
[15] C. Schneider, J. Sühnel, A molecular dynamics simulation of the flavin mononucleotide–RNA aptamer complex, Biopolymers 50 (1999) 287–302.
[16] D.H. Nguyen, S.C. DeFina, W.H. Fink, T. Dieckmann, Binding to an RNA aptamer changes the charge distribution and conformation of malachite green, J. Am. Chem. Soc. 124 (2002) 15081–15084.
[17] T. Dieckmann, S.E. Butcher, M. Sassanfar, J.W. Szostak, J. Feigon, Mutant ATP-binding RNA aptamers reveal the structural basis for ligand binding, J. Mol. Biol. 273 (1997) 467–478.
[18] D.H. Nguyen, T. Dieckmann, M.E. Colvin, W.H. Fink, Dynamics studies of a malachite green–RNA complex revealing the origin of the red-shift and energetic contributions of stacking interactions, J. Phys. Chem. B 108 (2004) 1279–1286.
[19] C.M. Reyes, P.A. Kollman, Structure and thermodynamics of RNA-protein binding: using molecular dynamics and free energy analyses to calculate the free energies of binding, J. Mol. Biol. 297 (2000) 1145–1158.
[20] V. Tsui, D.A. Case, Calculations of the absolute free energies of binding between RNA and metal ions using molecular dynamics simulations and continuum electrostatics, J. Phys. Chem. B 105 (2001) 11314–11325.
[21] A. Vaiana, E. Westhof, P. Auffinger, A molecular dynamics simulation study of an aminoglycoside/A-site RNA complex: conformational and hydration patterns, Biochimie 88 (2006) 1061–1073.
[22] T.E. Edwards, A.R. Ferré-D'Amaré, Crystal structures of the Thi-box riboswitch bound to thiamine pyrophosphate analogs reveal adaptive RNA-small molecule recognition, Structure 14 (2006) 1459–1468.
[23] C.D. Stoddard, S.D. Gilbert, R.T. Batey, Ligand-dependent folding of the three-way junction in the purine riboswitch, RNA 14 (2008) 675–684.
[24] M.J. Frisch, G.W. Trucks, H.B. Schlegel, G.E. Scuseria, M.A. Robb, J.R. Cheeseman, J.A. Montgomery Jr., T. Vreven, K.N. Kudin, J.C. Burant, J.M. Millam, S.S. Iyengar, J. Tomasi, V. Barone, B. Mennucci, M. Cossi, G. Scalmani, N. Rega, G.A. Petersson, H. Nakatsuji, M. Hada, M. Ehara, K. Toyota, R. Fukuda, J. Hasegawa, M. Ishida, T. Nakajima, Y. Honda, O. Kitao, H. Nakai, M. Klene, X. Li, J.E. Knox, H.P. Hratchian, J.B. Cross, V. Bakken, C. Adamo, J. Jaramillo, R. Gomperts, R.E. Stratmann, O. Yazyev, A.J. Austin, R. Cammi, C. Pomelli, J.W. Ochterski, P.Y. Ayala, K. Morokuma, G.A. Voth, P. Salvador, J.J. Dannenberg, V.G. Zakrzewski, S. Dapprich, A.D. Daniels, M.C. Strain, O. Farkas, D.K. Malick, A.D. Rabuck, K. Raghavachari, J.B. Foresman, J.V. Ortiz, Q. Cui, A.G. Baboul, S. Clifford, J. Cioslowski, B.B. Stefanov, G. Liu, A. Liashenko, P. Piskorz, I. Komaromi, R.L. Martin, D.J. Fox, T. Keith, M.A. Al-Laham, C.Y. Peng, A. Nanayakkara, M. Challacombe, P.M.W. Gill, B. Johnson, W. Chen, M.W. Wong, C. Gonzalez, J.A. Pople, Gaussian 03, Revision C. 02, Gaussian, Inc., Wallingford CT, 2004.
[25] G.M. Morris, D.S. Goodsell, R.S. Halliday, R. Huey, W.E. Hart, R.K. Belew, A.J. Olson, Automated docking using a Lamarckian genetic algorithm and an empirical binding free energy function, J. Comput. Chem. 19 (1998) 1639–1662.
[26] R. Huey, G.M. Morris, A.J. Olson, D.S. Goodsell, Software news and update a semiempirical free energy force field with charge-based desolvation, J. Comput. Chem. 28 (2007) 1145–1152.
[27] R. Odžak, M. Čalić, T. Hrenar, I. Primožič, Z. Kovarik, Evaluation of monoquaternary pyrimidium oximes potency to reactive tabun-inhibited human acetylcholinesterase, Toxicology 233 (2007) 85–96.
[28] G.X. Liu, Z.S. Zhang, X.M. Luo, J.H. Shen, H. Liu, X. Shen, K.X. Chen, H.L. Jiang, Inhibitory mode of indole-2-carboxamide derivatives against HLGPa: molecular docking and 3D-QSAR analyses, Bioorg. Med. Chem. 12 (2004) 4147–4157.
[29] A. Villa, E. Widjajakusuma, G. Stock, Molecular dynamics simulation of the structure, dynamics, and thermostability of the RNA hairpins uCACGg and cUUCGg, J. Phys. Chem. B 112 (2008) 134–142.
[30] K. Ziolkowska, P. Derreumaux, M. Folichon, O. Pellegrini, P. Régnier, I.V. Boni, E. Hajnsdorf, Hfq variant with altered RNA binding functions, Nucl. Acids Res. 34 (2006) 709–720.
[31] D. Van Der Spoel, E. Lindahl, B. Hess, G. Groenhof, A.E. Mark, H.J.C. Berendsen, GROMACS: fast, flexible and free, J. Comput. Chem. 26 (2005) 1701–1718.
[32] J. Wang, P. Cieplak, P.A. Kollman, How well does a restrained electrostatic potential (RESP) model perform in calculating conformational energies of organic and biological molecules? J. Comput. Chem. 21 (2000) 1049–1074.
[33] J. Wang, W. Wang, P.A. Kollman, D.A. Case, Automatic atom type and bond type perception in molecular mechanical calculations, J. Mol. Graphics Modell. 25 (2006) 247–260.
[34] J. Wang, R.M. Wolf, J.W. Caldwell, P.A. Kollman, D.A. Case, Development and testing of a general amber force field, J. Comput. Chem. 25 (2004) 1157–1174.
[35] D.L. Mobley, J.D. Chodera, K.A. Dill, On the use of orientational restraints and symmetry corrections in alchemical free energy calculations, J. Chem. Phys. 125 (2006) 084902.
[36] Y.G. Yingling, B.A. Shapiro, Dynamic behavior of the telomerase RNA hairpin structure and its relationship to dyskeratosis congenital, J. Mol. Biol. 348 (2005) 27–42.
[37] J. Eargle, A.A. Black, A. Sethi, L.G. Trabuco, Z. Luthey-Schulten, Dynamics of recognition between tRNA and elongation factor Tu, J. Mol. Biol. 377 (2008) 1382–1405.
[38] E.F. Healy, J. Sanders, P.J. King, W. Edward Robinson Jr., A docking study of L-chicoric acid with HIV-1 integrase, J. Mol. Graphics Modell. 27 (2009) 584–589.